Microbial Cell Factories

RESEARCH

Open Access

Bacterial biosynthesis of abietane-type diterpene ferruginol from glucose

Hyun Jeong Lee[1], Chaeyeon Kim[1,2], Yu Been Heo[1,2], Seong-Eun Kim[1,2] and Han Min Woo[1,2,3*]

Abstract

Background Microbial supply of plant extracts is a promising biomanufacturing strategy that requires engineering of metabolic pathways and enzymes. This study presents the engineering of *Corynebacterium glutamicum* for heterologous production of diterpenes miltiradiene and ferruginol.

Results Through targeted metabolic pathway modifications, including inactivation of pyruvate carboxylase and phytoene synthase, the HL01 strain was optimized to enhance pyruvate and geranylgeranyl pyrophosphate (GGPP) pools. Overexpression of key MEP pathway enzymes (Dxs and Idi) and implementation of three GGPP synthase modules further boosted diterpene synthesis. Then, combining those modules with diterpene synthase (DiTPS) and intact P450 reductase modules (CYP76AH1 and CPR1) enabled production of miltiradiene (ferruginol equivalent) at 237.46 ± 34.8 mg/L and ferruginol at 107.34 ± 1.2 mg/L under constant glucose feeding, respectively.

Conclusions Modular gene expression for heterologous metabolic pathway can be optimized for bacterial biosynthesis. This is the first demonstration of ferruginol production in bacteria. These findings pave the way for further optimization of diterpene biosynthesis through pathway engineering and module integration in bacterial systems.

Keywords Ferruginol, CRISPR, Corynebacterium glutamicum, P450, Metabolic engineering

Introduction

Ferruginol ($C_{20}H_{30}O$), an abietane-type tricyclic diterpene, is naturally obtained from the bark and roots of Chinese medicinal herb *Salvia miltiorrhiza* that has been widely used for the treatment of cerebrovascular and cardiovascular diseases for hundreds of years [1, 2]. Known for its valuable pharmacological properties, including anticancer activity [3], the sustainable production of diterpenes including ferruginol has garnered significant attention. However, traditional plant-based extraction methods are hindered by low yields, while climate change impacts plant cultivation, leading to supply instabilities [4]. Recent metabolic engineering and synthetic biology have demonstrated potential sustainable production of the diterpenes to overcome the limited supply [5, 6]. In addition, bacterial Cytochrome P450s (CYPs) using a kaurene-scaffold have facilitated high-throughput exploration of terpenoids and their chemical diversification [7]. This systematic approach could be beneficial to develop various bacterial cell factories for CYP-mediated products.

*Correspondence:
Han Min Woo
hmwoo@skku.edu
[1]BioFoundry Research Center, Institute of Biotechnology and Bioengineering, Sungkyunkwan University (SKKU), 2066 Seobu-ro, Jangan-gu, Suwon 16419, Republic of Korea
[2]Department of Food Science and Biotechnology, Sungkyunkwan University (SKKU), 2066 Seobu-ro, Jangan-gu, Suwon 16419, Republic of Korea
[3]Department of MetaBioHealth, Sungkyunkwan University (SKKU), 2066 Seobu-ro, Jangan-gu, Suwon 16419, Republic of Korea

To biosynthesize ferruginol and its derivatives such as carnosic acid [1], forskolin [8], or tanshinones [9], microbial systems, including yeasts and bacteria, require the development of heterologous metabolic pathway engineering to optimize the mevalonate pathway or the methylerythritol 4-phosphate (MEP) pathway for efficient isopentenyl diphosphate (IPP) supply. Additionally, the expression of plant-derived enzymes is essential for constructing diterpene backbones and producing oxidized diterpenes [7]. Specifically, for production of ferruginol, geranylgeranyl pyrophosphate (GGPP) synthase combines one dimethylallyl diphosphate (DMAPP) and three IPP units to produce GGPP (Fig. 1) [10–12]. The cyclization of GGPP to copalyl diphosphate (CPP) is catalyzed by class II terpene synthase (CPS). This is followed by further cyclization of CPP, initiated by class I terpene synthase, specifically kaurene synthase-like enzymes, leading to the formation of tricyclic miltiradiene. Subsequently, ferruginol and its derivatives are produced through oxidation mediated by CYP enzymes.

For microbial supply of diterpenes and its oxidized products, *Saccharomyces cerevisiae* has been engineered to overproduce miltiradiene [10, 11, 13], ferruginol [8, 14], carnosic acid [1, 12, 15], forskolin [8], and tanshinones [9]. Similarly, engineered *Escherichia coli* have been demonstrated heterologous production of taxadiene and its oxidized derivative, taxadien-5α-ol [16, 17]. *E. coli* has been utilized to biosynthesize kaurene and its oxidized product, steviol [18]. Regardless of species and strains, the production of diterpenes and their oxidized derivatives primarily depends on the optimization of key factors. These include enhancing the metabolic pathway for IPP supply, achieving efficient terpene synthase expression through optimized truncation of the protein sequence or metabolite channeling, and identifying specific pairs of CYP enzymes and their cognate CYP reductases (CPR). However, no studies to date have reported the production of miltiradiene or its oxidized derivatives in *E. coli* or other bacterial systems.

Corynebacterium glutamicum, a non-pathogenic industrial host widely used for amino acid production, has been extensively studied as one of microbial cell factories for the production of both natural products (natural-inherent; natural-noninherent) and non-natural products (non-natural-noninherent; non-natural-created) [19, 20]. Amino acids, diamines, alcohols, organic acids, biopolymers, and terpenoids have been produced in metabolically engineered *C. glutamicum*. In addition, strain-specific genetic tools have been developed to facilitate host engineering [21, 22], alongside synthetic expression vectors and modular DNA parts [23]. Furthermore, *C. glutamicum* exhibits low susceptibility to phages, thanks to the development of the prophage-free strain *C. glutamicum* MB001, which lacks three prophages (CGP1, CGP2, and CGP3) [24]. Thus, engineered *C. glutamicum* serves as a promising cell factory for the phage-free scale-up production of natural compounds, including terpenoids.

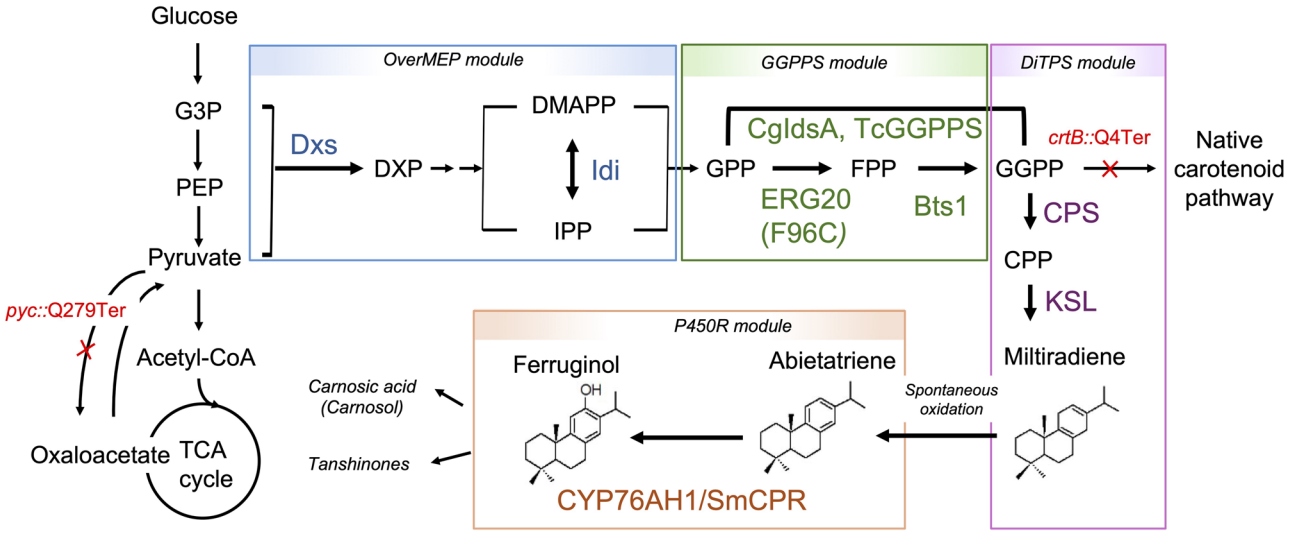

Fig. 1 Metabolic engineering for diterpene production in engineered *C. glutamicum*. The metabolic pathway for diterpene production in engineered *C. glutamicum* was divided into four distinct modules: OverMEP, GGPPS, DiTPS, and P450R. The parental strain, *C. glutamicum* HL01, was transformed with a series of plasmids, each encoding genes corresponding to these specific metabolic modules. The native *pyc* and *crtB* genes (shown in red) were inactivated in the strain HL01. See the Table 1 for the strains and plasmids used in this study. Abbreviations: Metabolite: G3P, glyceraldehyde 3-phosphate; Pyr, Pyruvate; DXP, 1-deoxy-D-xylulose 5-phosphate; IPP, isopentenyl diphosphate; DMAPP, dimethylallyl diphosphate; FPP, farnesyl diphosphate; GGPP, geranylgeranyl diphosphate; Enzyme: Dxs DXP synthase; Idi, isopentenyl diphosphate isomerase; GGPPS, Bts1, or IdsA, geranylgeranyl diphosphate synthase; ERG20(F96C), farnesyl diphosphate synthase; CPS, Class-II copalyl diphosphate synthase; KSL, Class-I kaurene synthase-like; CYP76AH1, cytochrome P450 oxidase; CPR, cytochrome P450 reductase

Therefore, in the present study, we metabolically engineered *C. glutamicum* to produce miltiradiene and ferruginol from glucose using a metabolic engineering approach to overcome the native metabolic pathway. In addition, we investigated whether combinatorial modular engineering to increase GGPP pools and to produce miltiradiene and ferruginol in *C. glutamicum*.

Methods

Bacterial strains and growth condition

E. coli DH5α [25] and *C. glutamicum* ATCC 13,032 (wild-type) were used in this study (Table 1). *E. coli* strains were grown in Lysogeny Broth (LB) medium (10 g/L tryptone, 5 g/L yeast extract, and 5 g/L NaCl) at 37 ºC on a rotary shaker at 200 rpm. When appropriate, the medium was supplemented with 30 μg/mL chloramphenicol or 50 μg/mL kanamycin. For strain development, *C. glutamicum* ATCC 13,032 and its derivatives were cultivated in brain heart infusion sorbitol-supplemented (BHIS) medium at 30 ºC on a rotary shaker at 120 rpm [21, 23]. When appropriate, the medium was supplemented with 7.5 μg/mL chloramphenicol, or 25 μg/mL kanamycin, and/or 50 μg/mL spectinomycin.

To construct gene inactivation mutants using the high-fidelity cytosine base editor for *C. glutamicum* (HF-CBE-STOP [21]), pCoryne-BE3-R132E was co-transformed to *C. glutamicum* WT with either pCoryne2-sgRNA-pyc(Q279Ter) or pCoryne2-sgRNA-crtB(Q4Ter), obtained from the laboratory sgRNA collection for *C. glutamicum*. After performing base editing to inactivate the *pyc* and *crtB* genes, we obtained the *C. glutamicum* HL01 strain and confirmed the genomic sequence at the targeted editing regions (Table 1). The various plasmids for gene expression for diterpene biosynthesis were introduced into *C. glutamicum* by electroporation, and strain validation was performed using colony PCR and DNA sequencing [26].

For diterpene production, *C. glutamicum* ATCC 13,032 derivative strains were pre-cultivated overnight in Brain Heart Infusion-supplemented with 91 g/L sorbitol (BHIS) medium at 30 °C and 250 rpm in 15 mL glass tubes. Following pre-cultivation, the strains were transferred to a baffled 96-deep well plate (DWP; Tomas Scientific, NJ, USA) and incubated aerobically at 30 °C and 1200 rpm in 0.6 mL of CgXII defined medium per well, containing 2% (w/v) glucose as the initial carbon source [27]. The DWP was covered with a gas-permeable sealing film (AeraSeal, Excel Scientific, Inc., CA, USA) to prevent contamination and to allow uniform gas exchange. When necessary, the medium was supplemented with 7.5 μg/mL of chloramphenicol (Cm), or 50 μg/mL of kanamycin (Km). Cell cultivation was carried out with the addition of 1 mM isopropyl β-D-1-thiogalactopyranoside (IPTG) to induce gene expression for diterpene production, introduced 4 h after inoculation.

Table 1 Bacteria strains and plasmids used in this study

Strain or plasmid	Relevant characteristics	References
Strains		
E. coli HIT-DH5α	F^{-}(80d *lac*Z M15) (*lac*ZYA-*arg*F) U169 *hsd*R17(r^{-} m^{+}) *rec*A1 *end*A1 *rel*A1 *deo*R96	RBC Bioscience
C. glutamicum WT	Wild type strain, biotin auxotroph, ATCC 13,032	ATCC
C. glutamicum HL01	ATCC 13,032 derivative, *pyc*::Q279Ter *crtB*::Q4Ter	This study
Plasmid		
pBbEB1c-RFP	ColE1 (*E.c.*), pBL1 (*C.g.*), lacI^{q} -P*trc*, BglBrick site, *rfp*, CoryneBrick vector, Cm^{r}	[23]
pTc*t*GGPPS-DI	pBbEB1c-RFP derivative carrying the truncated *GGPPS* gene(co) of *Taxus candensis* and carrying the native *dxs*, *idi* gene, Cm^{r}	This study
pIdsA-DI	pBbEB1c-RFP carrying the native *idsA*, *dxs*, *idi* gene, Cm^{r}	This study
pBE-DI	pBbEB1c-RFP carrying the *bts1*[GGGS]*Erg20(F96C)* gene(co) of *Saccharomyces cerevisiae* and native *dxs*, *idi* gene, Cm^{r}	This study
pBbEC1k-RFP	ColE1 (*E.c.*), pCG1 (*C.g.*), lacI^{q} -P*trc*, BglBrick site, *rfp*, CoryneBrick vector, Km^{r}	Lab plasmid
pKC	pBbEC1k-RFP derivative carrying the *KSL1*, *CPS1* genes(co) of *Salvia miltiorrhiza*, Km^{r}	This study
pCK	pBbEC1k-RFP derivative carrying the *CPS1*, *KSL1* genes(co) of *S. miltiorrhiza*, Km^{r}	This study
p*tKtC*	pBbEC1k-RFP derivative carrying the truncated *KSL1*[GGGS]*CPS1* gene(co) of *S. miltiorrhiza*, Km^{r}	This study
p*tKtC*-C^{P450}C^{R}	pBbEC1k-RFP derivative carrying the truncated *KSL1*[GGGS]*CPS1* gene(co) of *S. miltiorrhiza* and carrying the *CYP76AH1*, *CPR1* gene of *S. miltiorrhiza*, Km^{r}	This study
p*tKtC*-*tC*^{P450}*tC*^{R}	pBbEC1k-RFP derivative carrying the truncated *KSL1*[GGGS]*CPS1*gene of *S. miltiorrhiza* and carrying the truncated *CYP76AH1*, truncated *CPR1* gene of *S. miltiorrhiza*, Km^{r}	This study
pC^{P450}-eGFP	pBbEC1k-RFP derivative carrying the *CYP76AH1*of *S. miltiorrhiza* fused with *egfp*, Km^{r}	This study
p*tC*^{P450}-eGFP	pBbEC1k-RFP derivative carrying the truncated *CYP76AH1*of *S. miltiorrhiza* fused with *egfp*, Km^{r}	This study

Note (co) represents that the gene sequence is codon-optimized to *C. glutamicum* ATCC 13,032

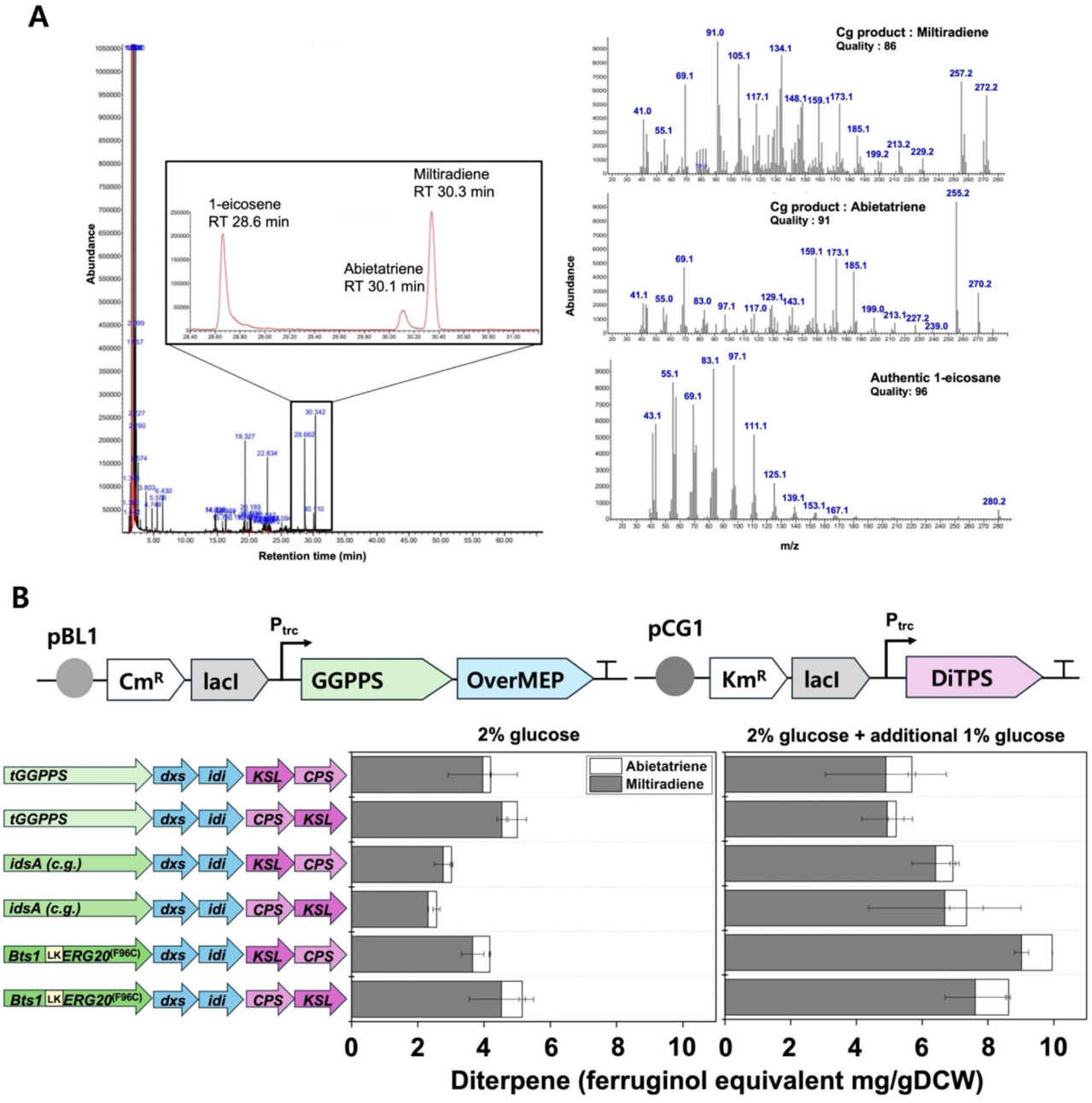

Fig. 2 Quantification of miltiradiene and abietatriene in engineered *C. glutamicum*. (**A**) GC-MS measurement of miltiradiene ($C_{20}H_{32}$) and abietatriene ($C_{20}H_{30}$) produced in engineered *C. glutamicum*. 1-eicosene ($C_{20}H_{40}$) was injected into sample as internal standard and ferruginol was used for quantification of miltiradiene and abietatriene (ferruginol equivalent mg/gDCW). (**B**) Heterologous diterpenes (miltiradiene and abietatriene) were produced in engineered *C. glutamicum* strains harboring various plasmids. A two-plasmid system was used for gene expressions: a pBL1-origin vector harboring GGPPS and OverMEP modules and a pCG1-origin vector harboring DiTPS module. Miltiradiene (grey) and abietatriene (white) were quantified as ferruginol equivalent mg/gDCW using GC-FID. Data represent mean values of at least triplicated cultivations, and error bars represent standard deviations. LK stands for a linker

Plasmid construction

All of the plasmids used for in this study were listed in Table 1. For the supplying GGPP pools (GGPPS module), *idsA* gene was PCR-amplified from the genomic DNA of *C. glutamicum*. Also, the truncated GGPPS gene [28] from *Taxus candensis*, in which hydrophobic N-terminal 294 amino-acid residues for soluble expression and *Bts1*-[GGT GGT GGT TCC]-*ERG20*(F96C) genes [29, 30] from *S. cerevisiae* were codon-optimized for *C. glutamicum* (Genscript) and were cloned into a CoryneBrick vector [23]. To overexpress key enzymes of the MEP pathway (OverMEP module, DI), the *dxs* gene, the

idi gene from *C. glutamicum*, were cloned into the plasmid (pTc*t*GGPPS or pIdsA or pBE) using the standard BglBrick cloning method [23], yielding GGPPS-Over-MEP module plasmids (Table 1). For the biosynthesis of miltiradiene (DiTPS module), the *KSL1* and *CPS1* genes [11] from *S. miltiorrhiza* were codon-optimized for *C. glutamicum* (Genscript, USA) and were cloned into a high-copy origin CoryneBrick vector (pBbEC1k-RFP), resulting in plasmids pKC and pCK. A KSL and CPS were fused together with a GGGS linker [11]. Additionally, truncated versions of the *KSL* and *CPS* genes was also cloned into a pBbEC1k-RFP, yielding p*tK*t*C*. Truncations of KSL and CPS were performed, removing amino acids M1 to C47 in SmKSL and M1 to S35 in SmCPS, respectively. A start codon (ATG) was introduced to ensure proper translation of the truncated versions. DNA sequences used in this study available in Supplementary Table S1.

For biosynthesis of ferruginol (P450R module), the *CYP76AH1* (GenBank accession no. JX422213) and *CPR1* (no. CBX24555) genes [14] from *S. miltiorrhiza* were codon-optimized for *C. glutamicum* (Genscript, USA) and they were cloned into a plasmid p*tK*t*C*, yielding p*tK*t*C*-C^{P450}C^{R}. Additionally, truncated *CYP76AH1* (M1-F22) and SmCPR (M1-W60) gene were modified, constructing p*tK*t*C*-*t*C^{P450}*t*C^{R}. Transmembrane helices of CYP76AH1 and SmCPR were predicted by the TMHMM 2.0 [31] (Supplementary Fig. S1). A start codon (ATG) was introduced to ensure proper translation of the truncated versions.

To investigate the localization of CYPs in *C. glutamicum*, the *CYP76AH1* gene and a truncated version of *CYP76AH1* (M1-F22) were cloned into the vector pBbEC1k-RFP. The *egfp* gene [23] was fused to both the *CYP76AH1* and truncated *CYP76AH1* genes by removing the stop codon of *CYP76AH1* and the start codon of *egfp*, generating pC^{P450}-eGFP and p*t*C^{P450}-eGFP, respectively.

Quantification of miltiradiene, abietatriene, and ferruginol

Cultured cells (1 mL) were harvested by centrifugation at 3600 × g for 10 min. After discarding the supernatant, the cell pellets were washed with distilled water. For extraction, the cell pellets were resuspended in 1 mL of distilled water. Subsequently, 1 mL of hexane (spiked with 1-eicosene as an internal standard at a final concentration of 10 mg/L) was added to the sample. The mixture was then transferred to 2 mL screw-top tubes containing 250 mg of glass beads (150–212 µm; Sigma-Aldrich). After disrupting the cells using a bead beater (Taco™ Prep, GeneReach Biotechnology Corp., Taichung City, Taiwan), the extraction mixture was centrifuged at 3600 × g for 10 min, and the supernatant from hexane layer was collected for further analysis. The sample was identified and quantified by both gas chromatography-mass spectrometry (GC-MS) and GC-Flame Ionization Detector (FID). In particular, GC-FID was employed for routine analyses after GC-MS analysis. GC-MS (Agilent 5977B GC/MSD) is equipped with an Agilent HP-5MS column (30 m × 0.25 mm, thickness 0.25 µm): Carrier gas, He (1 mL/min). The initial oven temperature was set at 50 °C followed by a 40 °C/min gradient to 170 °C, and 20 °C/min in gradient to 240 °C, 40 °C /min gradient to 300 °C, and a final 1 min hold. The mass spectrometer was operated at 70 eV with selected ion monitoring (SIM), and the mass range was m/z 29 – 300. The ion source temperature was maintained at 230 °C. GC-FID (Agilent 7890B, Waldbronn, Germany) is equipped with an Agilent 122–5032 DB-5 column (30 m × 0.2 mm, thickness 0.11 µm): Carrier gas, N_2 (1mL/min). The initial oven temperature was set at 50 °C for 2 min followed by a 40 °C/min gradient to 170 °C, and 20 °C/min in gradient to 240 °C, 40 °C /min gradient to 300 °C, and a final 1 min hold.

After GC analysis, the concentrations of miltiradiene and abietatriene were determined by converting their peak areas to ferruginol equivalent normalized by internal standard, using a standard curve prepared with ferruginol (Merck, USA) (CAS:3452-07-01, Cat.: 184411). For quantification of ferruginol, an authentic standard of ferruginol (CAS: 514-62-5, Cat.: TBZ2395), purchased from ChemFaces (Wuhan, China), was utilized to generate a corresponding standard curve.

Quantification of glucose

Glucose in the supernatant was quantified using high-performance liquid chromatography (HPLC) as described previously [32]. Briefly, the culture supernatant was passed through a syringe filter (pore size = 0.45 μm). The concentation of glucose was detected by a HPLC (Agilent 1260, Waldbronn, Germany) equipped with refractive index detector (RID) and a Hi-Plex H, 7.7 × 300 mm column (Agilent Technologies) under the following conditions: sample volume of 20 µL, mobile phase of 5 mM H_2SO_4, flow rate of 0.6 mL/min, and column temperature of 65 °C.

Confocal microscopy

Cells were cultivated in the CgXII medium with 2% (w/v) glucose and harvested 48 h after inoculation. After harvesting, the cells were washed three times with 6.5 mM phosphate-buffered saline (PBS, pH 7.4) and resuspended in the same buffer. To immobilize the cells and prevent movement, the suspension was mixed with 0.25% agarose. The prepared samples were then imaged using a confocal microscope (Zeiss LSM 980 laser scanning microscope with Airyscan 2 module, Zeiss, Germany) with an excitation filter at 490 nm and an emission filter at 520 nm. Images were acquired and processed using ZEN software.

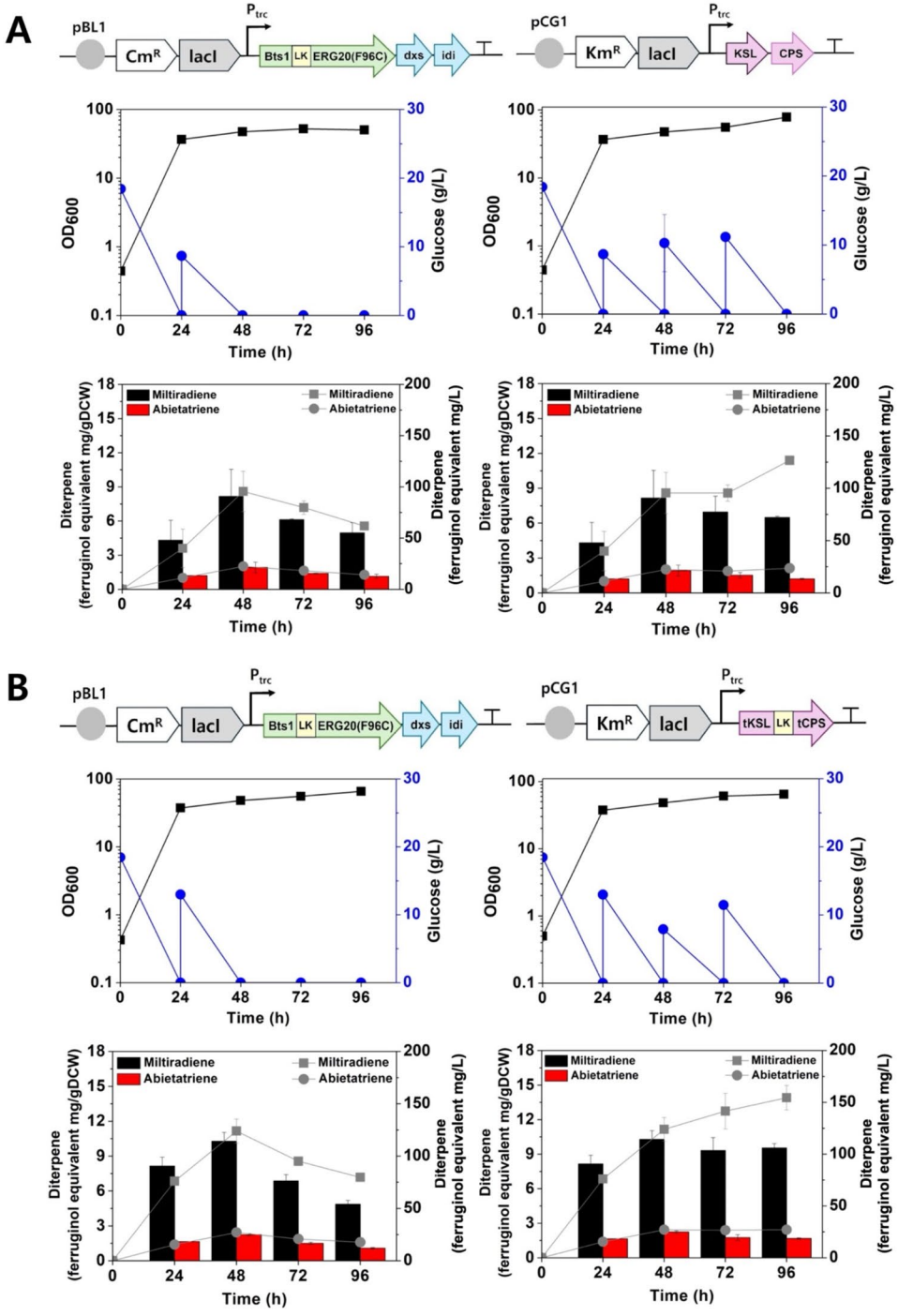

Fig. 3 Miltiradiene and abietatriene productions in engineered *C. glutamicum* (**A**) A fed-batch cultivation of engineered strains (*C. glutamicum* HL01 harboring pBE-DI pKC) was conducted, starting with 2% (w/v) initial glucose, followed by a single glucose supplementation (1%, w/v) during the cultivation (left panel). Optical densities at 600 nm (OD_{600}, black square) and glucose concentrations (g/L, blue circle) in the medium were measured (upper panel). Relative diterpene contents (ferruginol equivalent mg/gDCW) and concentrations (ferruginol equivalent mg/L) profiles were measured for miltiradiene (black bar, square symbol) and abietatriene (red bar, circle symbol), respectively (lower panel). A fed-batch cultivation of the engineered strain was conducted, starting with 2% (w/v) initial glucose, followed by multiple glucose supplementations (1%, w/v) during the cultivation (right panel). Data represent mean values of at least triplicated cultivations, and error bars represent standard deviations. (**B**) A fed-batch cultivation of engineered strains (*C. glutamicum* HL01 harboring pBE-DI p*tKtC*) was conducted with truncation versions of KSL and CPS. LK stands for a linker. See the details above

Results and discussion

Synthetic metabolic pathway modules in *C. glutamicum* for diterpene productions

Previously, we demonstrated that inactivating both the

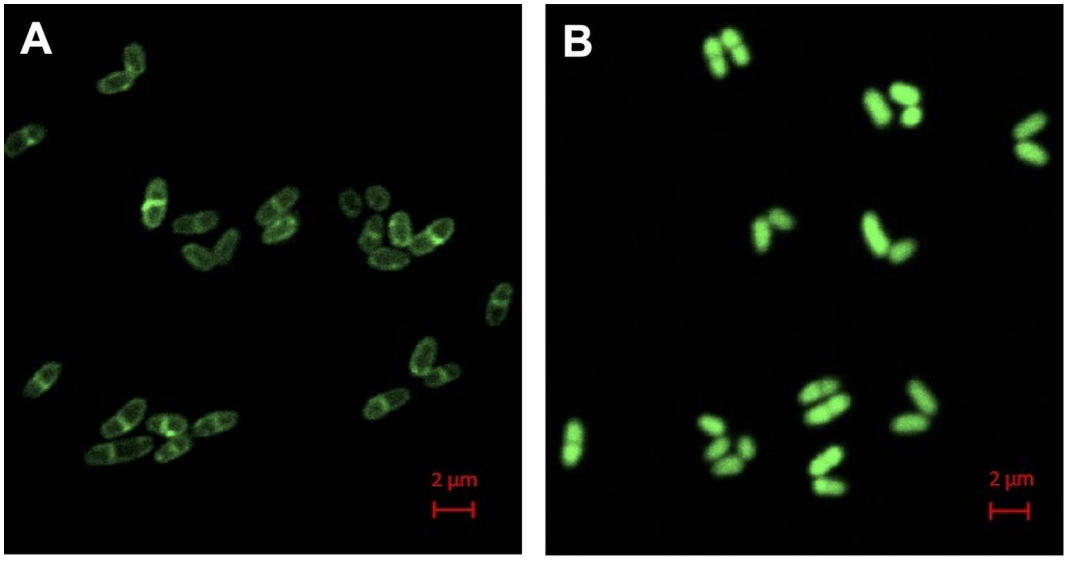

Fig. 4 Confocal microscopy analysis of Cytochrome CYP76AH1 expression in engineered *C. glutamicum*. The *C. glutamicum* HL01 strains harboring a plasmid of either pC^{P450}-eGFP (**A**) or pt*C*^{P450}-eGFP (**B**) were prepared. Fluorescence imaging was performed using a Zeiss LSM 980 laser scanning microscope equipped with an Airyscan 2 module (Zeiss, Germany). Images were acquired and processed with ZEN software, utilizing an excitation filter at 490 nm and an emission filter at 520 nm. Scale bar is 2 µm

pyruvate carboxylase (PC), which converts pyruvate to oxaloacetate, and the major geranylgeranyl pyrophosphate synthase (IdsA), which competes with squalene synthase, significantly increased triterpene squalene production in *C. glutamicum* [32, 33]. Similarly, for diterpene production, the native metabolic pathway of *C. glutamicum* was engineered to enhance the pools of pyruvate and geranylgeranyl pyrophosphate (GGPP) instead of farnesyl pyrophosphate (FPP). This was achieved by inactivating the *pyc* gene (*pyc*::Q279Ter) encoding PC and the *crtB* gene (*crtB*::Q4Ter) encoding phytoene synthase (an enzyme that converts GGPP to phytoene) using a cytosine base editor [21]. The base editor introduced premature translational termination codons in these target genes. This engineering resulted in the construction of strain HL01 (Table 1).

Next, to further enhance the pools of isopentenyl pyrophosphate (IPP) biosynthesized from glyceraldehyde 3-phospahte and pyruvate, a C5 isoprenoid building block for diterpene synthesis, we overexpressed key enzymes of the methylerythritol 4-phosphate (MEP) pathway [32, 34, 35]. In the OverMEP module, Dxs (1-deoxy-xylulose-5-phosphate synthase) and Idi (isopentenyl diphosphate isomerase) were selected for overexpression in *C. glutamicum* HL01 (Fig. 1). To synthesize geranylgeranyl pyrophosphate (GGPP), the substrate for diterpene synthase derived from IPP, we developed three distinct GGPP synthase (GGPPS) modules. The first GGPPS module involved the overexpression of the native *idsA* gene, which is known as the primary GGPPS in *C. glutamicum* and exhibits high catalytic efficiency with DMAPP and IPP [36]. The second GGPPS module featured the co-expression of GGPPS from Canadian yew *Taxus canadensis* (used for production of taxanes), which has been utilized for diterpene levopimaradiene production in *E. coli* [37]. The third GGPPS module utilized a fusion protein of Bts1 and the ERG20(F96C) variant [29], which has been previously expressed in *S. cerevisiae* for miltiradiene production and demonstrated significant improvements in production efficiency [11]. To optimize this system for *C. glutamicum*, we constructed a codon-optimized Bts1-ERG20(F96C) fusion GGPPS. In combination with the OverMEP and GGPPS modules, we constructed three distinct plasmids: pTc*t*GGPPS-DI, pIdsA-DI, and pBE-DI.

The DiTPS and P450R modules were designed to enable the biosynthesis of ferruginol from GGPP. The DiTPS module facilitates the conversion of GGPP to miltiradiene using diterpene synthase, while the P450R module catalyzes the hydroxylation of miltiradiene via CYP monooxygenase in conjunction with a CYP reductase. In the DiTPS module, we selected the CPS gene, encoding copalyl diphosphate synthase, and the KSL gene, encoding a kaurene synthase-like enzyme, both derived from the Chinese medicinal herb *S. miltiorrhiza* [11]. Subsequently, we evaluated different expression orders of KSL and CPS to optimize their functionality because different translational order in an operon could cause slightly different protein abundance in a host. The first gene has more time for translation then the second gene [38]. We constructed two different versions of the plasmid: pKC and pCK. In the P450R module, the CYP76AH1 and SmCPR genes from *S. miltiorrhiza*, which have been demonstrated to facilitate ferruginol production in yeast

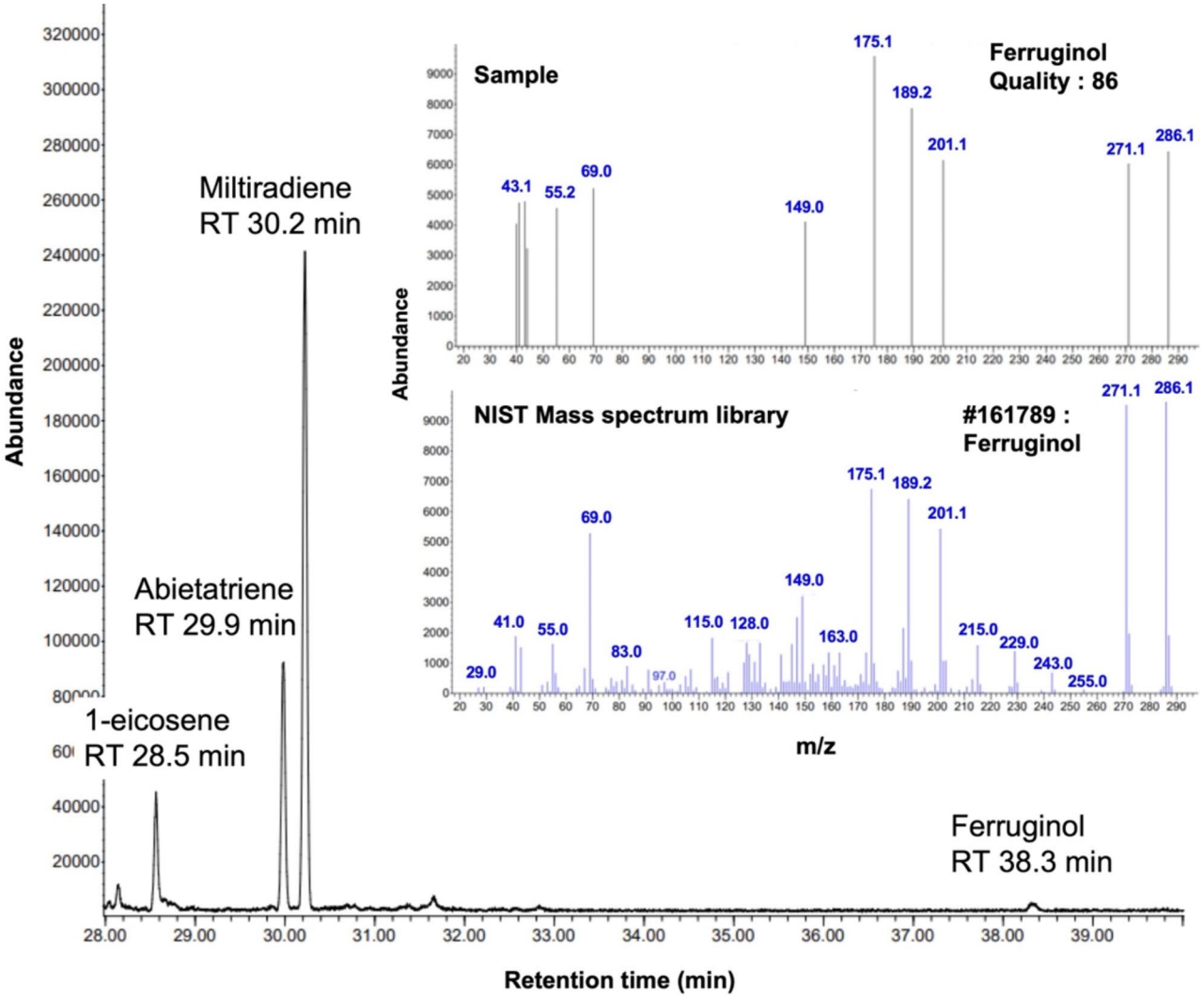

Fig. 5 Identification of ferruginol produced in engineered *C. glutamicum* The chromatographic profile and mass fragments of the sample were analyzed using GC-MS. The sample was extracted from engineered cells, and the mass fragment ions (m/z) obtained at retention time 38.3 min were compared with the NIST mass spectrum library (entry #161789, ferruginol)

systems [14], were integrated into the DiTPS module to produce ferruginol from GGPP.

Heterologous production of miltiradiene and abietatriene in engineered *C. glutamicum*

To produce the miltiradiene in *C. glutamicum*, we constructed the strain HL01 harboring two distinct vectors, representing six different combinations of the GGPPS, OverMEP, and DiTPS modules (Fig. 2). First, we cultivated the six strains using 2% (w/v) glucose as the sole carbon source for 48 h. Analysis of the extracted samples revealed the presence of a miltiradiene peak, along with a peak corresponding to abietatriene, a by-product formed through the spontaneous oxidation of miltiradiene (Fig. 2A). Subsequently, due to the unavailability of commercially purchased miltiradiene and abietatriene, we used ferruginol as a structurally relevant equivalent standard to quantify the relative levels of miltiradiene and abietatriene in the engineered strains. This approach enabled us to measure the relative levels of miltiradiene and abietatriene across the six module combinations (Fig. 2B). As a result, the combination of pBE-DI and pCK modules yielded 4.5 ± 1.0 mg miltiradiene (ferruginol equivalent) per gDCW and 0.63 ± 0.1 mg abietatriene (ferruginol equivalent) per gDCW in *C. glutamicum* HL01 at 48 h. Regardless of the module constructs, the abietatriene level consistently accounted for 19% of the miltiradiene level. Interestingly, the ratio of abietatriene to miltiradiene was higher in engineered *C. glutamicum* compared to engineered yeast [1, 11, 39]. This difference is likely attributed to the small-scale cultivation used in our study, which involved microplates agitated at 1200 rpm, providing higher oxygen levels that facilitated spontaneous oxidation. The GGPPS

module incorporating a fusion protein of Bts1 and the ERG20(F96C) variant demonstrated better miltiradiene production compared to other GGPPS modules (Student *t*-test, p-value < 0.05; Fig. S2). In the DiTPS module, the gene expression order of KSL and CPS did not significantly affect diterpene production (Fig. S2).

To investigate the impact of carbon source availability on production, 1% (w/v) glucose was added after the depletion of the initial 2% (w/v) glucose. This supplementation with an additional carbon source resulted in increased diterpene production. The combination of pBE-DI and pKC modules resulted in 7.61 ± 1.0 mg miltiradiene (ferruginol equivalent) per gDCW and 1.02 ± 0.05 mg abietatriene (ferruginol equivalent) per gDCW in *C. glutamicum* HL01. So, we selected *C. glutamicum* HL01 harboring pBE-DI and pKC as the diterpene-producing strain for the next improvement.

Improvement of diterpene production using constant glucose feeding

Since we observed increased diterpene production with additional glucose feeding, we implemented a fed-batch fermentation strategy to enhance diterpene yields [40, 41]. First, we measured cell growth and diterpene production (miltiradiene and abietatriene) in the *C. glutamicum* strain HL01 harboring pBE-DI and pKC plasmids during cultivation with a single glucose feeding (Fig. 3A). Interestingly, the titers and contents of miltiradiene and its derivative, abietatriene, decreased after glucose depletion during cultivation. *C. glutamicum* has cytochrome P450 enzymes involved in various oxidation reactions. For instance, certain aromatic oxygenases, such as cytochrome P450 hydroxylases, can oxidize compounds like indole at specific positions, leading to further oxidation products [42]. However, *C. glutamicum* lacks potential C_{20}-oxidases (CYPs) with promiscuous activity that could convert miltiradiene into oxygenated derivatives. Then, we speculated that miltiradiene undergoes non-enzymatic degradation during deep well plate cultivation at 1200 rpm, possibly driven by an unidentified mechanism. To direct carbon flux toward miltiradiene production and prevent glucose depletion in the cells, we implemented continuous glucose feeding into the medium. This approach resulted in an increase in the concentration of miltiradiene (ferruginol equivalent) at 126.7 ± 0.9 mg/L at 96 h, although the relative content of miltiradiene was slightly lower at that time point.

To further enhance the production titer, we investigated the channeling of GGPP to miltiradiene via CPP by expressing fused KSL and CPS enzymes. Additionally, we employed a truncated KSL (*t*KSL) lacking the chloroplast transit peptide (M1-C47) and a truncated CPS (*t*CPS) lacking the chloroplast transit peptide N-terminal region (M1-S35) to improve catalytic efficiency and promote soluble protein expression [10, 15]. This strategy has been demonstrated to benefit heterologous diterpene production by increasing the local concentration of intermediates through enhanced metabolic channeling. As a result, we observed a 1.26-fold increase in miltiradiene production at 48 h in *C. glutamicum* HL01 harboring pBE-DI and p*tKtC* (10.3 ± 0.8 ferruginol equivalent mg/gDCW), compared to *C. glutamicum* HL01 harboring pBE-DI and pKC (8.2 ± 2.4 ferruginol equivalent mg/gDCW) (Fig. 3B). With continuous glucose feeding, *C. glutamicum* HL01 harboring pBE-DI and p*tKtC* maintained consistent production throughout the cultivation period, achieving a final miltiradiene (ferruginol equivalent) titer of 154.5 ± 11.8 mg/L at 96 h. A 10% non-enzymatic degradation of miltiradiene and abietatriene occurred between 48 h and 96 h in *C. glutamicum* HL01 strain harboring pBE-DI p*tKtC*.

Heterologous production of ferruginol in *C. glutamicum*

Next, we sought to co-express the P450R module in *C. glutamicum* HL01 harboring pBE-DI and p*tKtC* for miltiradiene production. Among six CYP genes identified in the rhizome of *S. miltiorrhiza*, CYP76AH1 demonstrated catalytic activity in converting miltiradiene to ferruginol when co-expressed with CPR in *S. cerevisiae* [14]. Based on this, we selected the *CYP76AH1* gene and its cognate *CPR1* as the P450R module for ferruginol production in *C. glutamicum*. Additionally, we evaluated a truncated version of CYP76AH1 and SmCPR to enhance soluble expression and improve ferruginol production by testing either *C. glutamicum* HL01 pBE-DI p*tKtC*-$C^{P450}C^{R}$ or *C. glutamicum* HL01 pBE-DI p*tKtC*-*t*C^{P450}*t*C^{R}.

First, we tested whether the CYP76AH1 protein or its truncated version were expressed in the cytoplasmic membrane or the cytosol, respectively. A single transmembrane helix of CYP76AH1 was predicted (P5-F22; Fig. S1). To investigate its soluble expression, a truncated version of CYP76AH1, lacking the M1-F22 region and incorporating the start codon ATG, was expressed in the *C. glutamicum* wild-type. Confocal microscopy analysis confirmed that the intact CYP76AH1 was expressed in a membrane-associated manner, while the truncated CYP76AH1 protein was correctly localized to its intended cytosol. (Fig. 4). Subsequently, based on the transmembrane analysis using the TMHMM 2.0 [31], SmCPR was truncated by removing the M1-W60 region. The truncated version of SmCPR, incorporating the start codon ATG, was used for further production studies without confocal analysis, as its topology was simpler compared to CYP76AH1 (Fig. S1).

Next, we cultivated engineered strains (*C. glutamicum* HL01 pBE-DI p*tKtC*-$C^{P450}C^{R}$, a intact P450R module; *C. glutamicum* HL01 pBE-DI p*tKtC*-*t*C^{P450}*t*C^{R}, a truncated P450R module) with glucose as sole carbon source

and measured the diterpene and ferruginol productions throughout the cultivation period. As a result, ferruginol was successfully produced in engineered bacteria for the first time (Fig. 5). Notably, only the *C. glutamicum* HL01 strain harboring pBE-DI p*tKtC*-$C^{P450}C^{R}$ module produced ferruginol. In addition, the strain produced miltiradiene and abietatriene as well (Fig. 6). Then, we analyzed the relative production levels of diterpene and the absolute production levels of ferruginol in the heterologous metabolic pathway. Under both single and multiple glucose feeding conditions, the relative levels of miltiradiene produced in the ferruginol-producing strain were significantly decreased at 48 h (Fig. 6A), compared to the parental miltiradiene-producing strain (Fig. 3B). When we calculated the molar conversion of ferruginol from the abietatriene and miltiradiene contents quantified as ferruginol equivalent, we found that 13.0% of the diterpene contents was converted to ferruginol between 24 h and 96 h of cultivation (Fig. 6A). This conversion in *C. glutamicum* HL01 strain harboring pBE-DI p*tKtC*-$C^{P450}C^{R}$ was higher than the unidentified non-enzymatic degradation of abietatriene, which resulted in a 10% loss from 48 h to 96 h in *C. glutamicum* HL01 strain harboring pBE-DI p*tKtC* (Fig. 3B). The increase in ferruginol production was attributed to the catalytic activity of the P450R module, demonstrating a spontaneous oxidation-coupled enzymatic conversion of miltiradiene to ferruginol since the molar conversion of sole abietatriene to ferruginol exceeded 100% between 24 h and 96 h of cultivation.

Interestingly, the level of abietatriene in the ferruginol-producing strain was higher than that in the miltiradiene-producing strain, regardless of glucose feeding conditions. Co-expression of the intact P450R could promote spontaneous oxidation of miltiradiene to form abietatriene and catalyzes a single oxidation at C12 position of abietatriene to form ferruginol [14, 15, 43]. On the contrary, the strain carrying a truncated version of the P450R module (C. *glutamicum* HL01 pBE-DI p*tKtC*-*t*C^{P450}*t*C^{R}) did not produce ferruginol although lower miltiradiene levels and higher abietatriene levels (Fig. 6B) compared to the miltiradiene-producing strain (*C. glutamicum* HL01 harboring pBE-DI p*tKtC*) (Fig. 3B). Thus, ferruginol production requires a functional expression of the P450R module with its membrane association.

For ferruginol production, miltiradiene and abietatriene levels declined following glucose depletion after 48 h, whereas the level of ferruginol remained stable. Under constant glucose feeding, the level of ferruginol increased, reaching a content of 6.23 ± 0.2 mg/gDCW and a concentration of 107.34 ± 1.2 mg/L at 96 h (Fig. 6A). Further optimization on fermentation conditions and scale-up processes will be required to achieve feasible and efficient production of ferruginol in engineered *C. glutamicum*. Similarly, in an engineered yeast, the GGPPS, DiTPS, and P450R modules has been utilized with an optimized mevalonate pathway and led to a heterologous production of ferruginol at 10.5 mg/L in a flask scale [14]. Further pathway engineering of yeasts with various P450 expressions have allowed the carnosic acid productions [1, 15]. Systematic expression of bacterial CYPs and CPRs for diversifying terpene production [7], incorporation of functional compartmentalization to achieve targeted protein localization [44], and the application of metabolic channeling through protein fusions to enhance P450 reaction efficiency [45] have all been successfully demonstrated in bacteria. Leveraging these strategies in engineering *C. glutamicum* holds the potential to significantly enhance diterpene production and expand applications to the biosynthesis of other terpenoids.

Conclusions

In this study, we successfully developed a bacterial strain capable of heterologous miltiradiene production by incorporating the GGPPS, DiTPS, and OverMEP modules for the first time. Furthermore, the integration of heterologous membrane-associated plant P450 and reductase enzymes enabled the production of ferruginol in bacteria. Subsequent pathway engineering efforts, including the exploration of various P450 and reductase proteins, will focus on optimizing the sustainable production of natural diterpenes for biotechnological applications.

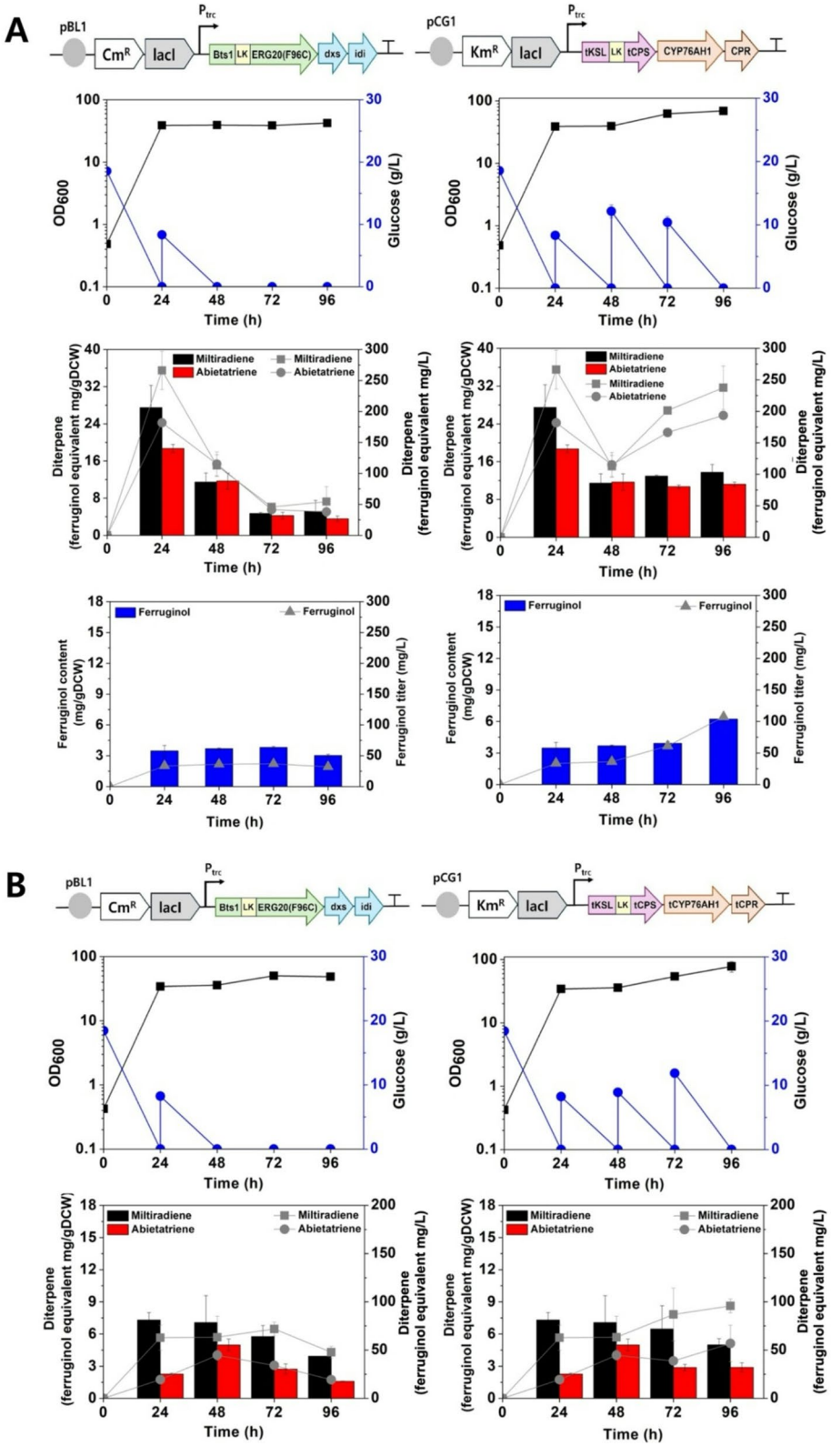

Fig. 6 (See legend on next page.)

(See figure on previous page.)

Fig. 6 Ferruginol production in engineered *C. glutamicum*. (**A**) A fed-batch cultivation of engineered strains (*C. glutamicum* HL01 harboring pBE-Dl p*tKt*C-$C^{P450}C^{R}$) was conducted, starting with 2% (w/v) initial glucose, followed by a single glucose supplementation (1%, w/v) during the cultivation (left panel). Optical densities at 600 nm (OD_{600}, black square) and glucose concentrations (g/L, blue circle) in the medium were measured. Relative diterpene contents (ferruginol equivalent mg/gDCW) profiles were measured for miltiradiene (black bar, square symbol) and abietatriene (red bar, circle symbol), respectively (left Y-axis). Ferruginol ($C_{20}H_{30}O$) content profiles were measured (mg/gDCW, blue bar, triangle symbol) (left Y-axis). Concentration of diterpene (ferruginol equivalent mg/L) and ferruginol (mg/L) profiles were measured, respectively (right Y-axis). A fed-batch cultivation of the engineered strain was conducted, starting with 2% (w/v) initial glucose, followed by multiple glucose supplementations (1%, w/v) during the cultivation (right panel). Data represent mean values of at least triplicated cultivations, and error bars represent standard deviations. (**B**) A fed-batch cultivation of engineered strains (*C. glutamicum* HL01 harboring pBE-Dl p*tKt*C-*t*C^{P450}*t*C^{R}) was conducted with truncation versions of CYP76AH1 and SmCPR. LK stands for a linker. See the details above

Supplementary Information

The online version contains supplementary material available at https://doi.org/10.1186/s12934-025-02691-3.

Supplementary Material 1

Acknowledgements
The authors thank to Jigyeong Son, Jun Sung Park, You Lim Lee for the technical support.

Author contributions
H.J.L. and H.M.W. designed the experiments, analyzed the data, and wrote the manuscript. H.J.L. and C. K. performed the experiments. H.J.L., C.K., Y.B.H., S.-E.K. and H.M.W. guided the scope of the project and provided critical input for the manuscript. All authors read and approved the final manuscript.

Funding
This study is supported by the National Research Foundation of Korea funded by the Korean Government (Ministry of Science and ICT) (RS-2022-NR070265 to HMW, 2022M3J5A1062990 to HMW, 2022R1A4A5032720 to HMW, RS-2022-NR067345 to HMW, 2021R1I1A1A01057622 to HJL).

Data availability
No datasets were generated or analysed during the current study.

Declarations

Ethics approval and consent to participate
Not applicable.

Consent for publication
Not applicable.

Competing interests
The authors declare no competing interests.

Received: 10 December 2024 / Accepted: 10 March 2025
Published online: 19 March 2025

References

1. Scheler U, Brandt W, Porzel A, Rothe K, Manzano D, Božić D, Papaefthimiou D, Balcke GU, Henning A, Lohse S, et al. Elucidation of the biosynthesis of carnosic acid and its reconstitution in yeast. Nat Commun. 2016;7:12942.
2. Bispo de Jesus M, Zambuzzi WF, Ruela de Sousa RR, Areche C, Santos de Souza AC, Aoyama H, Schmeda-Hirschmann G, Rodríguez JA, Monteiro, de Souza Brito AR, Peppelenbosch MP et al. Ferruginol suppresses survival signaling pathways in androgen-independent human prostate cancer cells. *Biochimie* 2008, 90:843–854.
3. Jassbi AR, Hadavand Mirzaei H, Firuzi O, Pirhadi S, Asadollahi M, Chandran JN, Schneider B. Cytotoxic abietane-type diterpenoids from roots of salvia spinosa and their in Silico pharmacophore modeling. Nat Prod Res. 2021;36:3183–8.
4. Che Sulaiman IS, Basri M, Fard Masoumi HR, Chee WJ, Ashari SE, Ismail M. Effects of temperature, time, and solvent ratio on the extraction of phenolic compounds and the anti-radical activity of *Clinacanthus nutans* Lindau leaves by response surface methodology. Chem Cent J. 2017;11:54.
5. Liu Y, Zhao X, Gan F, Chen X, Deng K, Crowe SA, Hudson GA, Belcher MS, Schmidt M, Astolfi MCT, et al. Complete biosynthesis of QS-21 in engineered yeast. Nature. 2024;629:937–44.
6. Ōhinata H, Inoue N, Yonei Y. Separation of antioxidative ferruginol from Japanese Cedar bark by supercritical carbon dioxide. In Developments Food Eng 1994: 843–5.
7. Lin G-M, Voigt CA. Design of a redox-proficient Escherichia coli for screening terpenoids and modifying cytochrome P450s. Nat Catal. 2023;6:1016–29.
8. Forman V, Bjerg-Jensen N, Dyekjær JD, Møller BL, Pateraki I. Engineering of CYP76AH15 can improve activity and specificity towards forskolin biosynthesis in yeast. Microb Cell Fact. 2018;17:181.
9. Ma Y, Cui G, Chen T, Ma X, Wang R, Jin B, Yang J, Kang L, Tang J, Lai C, et al. Expansion within the CYP71D subfamily drives the heterocyclization of Tanshinones synthesis in *Salvia miltiorrhiza*. Nat Commun. 2021;12:685.
10. Hu T, Zhou J, Tong Y, Su P, Li X, Liu Y, Liu N, Wu X, Zhang Y, Wang J, et al. Engineering chimeric diterpene synthases and isoprenoid biosynthetic pathways enables high-level production of miltiradiene in yeast. Metab Eng. 2020;60:87–96.
11. Zhou YJ, Gao W, Rong Q, Jin G, Chu H, Liu W, Yang W, Zhu Z, Li G, Zhu G, et al. Modular pathway engineering of diterpenoid synthases and the mevalonic acid pathway for miltiradiene production. J Am Chem Soc. 2012;134:3234–41.
12. Ignea C, Athanasakoglou A, Ioannou E, Georgantea P, Trikka FA, Loupassaki S, Roussis V, Makris AM, Kampranis SC. Carnosic acid biosynthesis elucidated by a synthetic biology platform. Proc Natl Acad Sci. 2016;113:3681–6.
13. Bai X, Wang S, Zhang Q, Hu Y, Zhou J, Men L, Li D, Ma J, Wei Q, Xu M, et al. Reprogramming the metabolism of yeast for High-Level production of miltiradiene. J Agric Food Chem. 2024;72:8704–14.
14. Guo J, Zhou YJ, Hillwig ML, Shen Y, Yang L, Wang Y, Zhang X, Liu W, Peters RJ, Chen X, et al. CYP76AH1 catalyzes turnover of miltiradiene in Tanshinones biosynthesis and enables heterologous production of ferruginol in yeasts. Proc Natl Acad Sci. 2013;110:12108–13.
15. Wei P, Zhang C, Bian X, Lu W. Metabolic engineering of *Saccharomyces cerevisiae* for heterologous carnosic acid production. Front Bioeng Biotechnol. 2022;10:916605.
16. Ajikumar PK, Xiao W-H, Tyo KEJ, Wang Y, Simeon F, Leonard E, Mucha O, Phon TH, Pfeifer B, Stephanopoulos G. Isoprenoid pathway optimization for taxol precursor overproduction in *Escherichia coli*. Science. 2010;330:70–4.
17. Biggs BW, Lim CG, Sagliani K, Shankar S, Stephanopoulos G, De Mey M, Ajikumar PK. Overcoming heterologous protein interdependency to optimize P450-mediated taxol precursor synthesis in *Escherichia coli*. Proc Natl Acad Sci. 2016;113:3209–14.
18. Sun Y, Chen Z, Wang G, Lv H, Mao Y, Ma K, Wang Y. De Novo production of versatile oxidized Kaurene diterpenes in *Escherichia coli*. Metab Eng. 2022;73:201–13.
19. Heider SAE, Wendisch VF. Engineering microbial cell factories: metabolic engineering of *Corynebacterium glutamicum* with a focus on non-natural products. Biotechnol J. 2015;10:1170–84.
20. Lee JW, Na D, Park JM, Lee J, Choi S, Lee SY. Systems metabolic engineering of microorganisms for natural and non-natural chemicals. Nat Chem Biol. 2012;8:536–46.
21. Heo YB, Hwang G-H, Kang SW, Bae S, Woo HM, Li W. High-Fidelity cytosine base editing in a GC-Rich *Corynebacterium glutamicum* with reduced DNA Off-Target editing effects. Microbiol Spec. 2022;10:e03760–03722.
22. Jiang Y, Qian F, Yang J, Liu Y, Dong F, Xu C, Sun B, Chen B, Xu X, Li Y, et al. CRISPR-Cpf1 assisted genome editing of *Corynebacterium glutamicum*. Nat Commun. 2017;8:15179.
23. Kang MK, Lee J, Um Y, Lee TS, Bott M, Park SJ, Woo HM. Synthetic biology platform of CoryneBrick vectors for gene expression in *Corynebacterium*

glutamicum and its application to xylose utilization. Appl Microbiol Biotechnol. 2014;98:5991–6002.
24. Baumgart M, Unthan S, Rückert C, Sivalingam J, Grünberger A, Kalinowski J, Bott M, Noack S, Frunzke J. Construction of a Prophage-Free variant of *Corynebacterium glutamicum* ATCC 13032 for use as a platform strain for basic research and industrial biotechnology. Appl Environ Microbiol. 2013;79:6006–15.
25. Hanahan D. Studies on transformation of *Escherichia coli* with plasmids. J Mol Biol. 1983;166:557–80.
26. Eggeling L, Bott M. Handbook of *Corynebacterium glutamicum*. CRC; 2005.
27. Kang DH, Ko SC, Heo YB, Lee HJ, Woo HM. RoboMoClo: A Robotics-Assisted modular cloning framework for multiple gene assembly in biofoundry. ACS Synth Biol. 2022;11:1336–48.
28. Burke C, Croteau R. Interaction with the small subunit of Geranyl diphosphate synthase modifies the chain length specificity of geranylgeranyl diphosphate synthase to produce Geranyl diphosphate. J BiolChem. 2002;277:3141–9.
29. Ignea C, Trikka FA, Nikolaidis AK, Georgantea P, Ioannou E, Loupassaki S, Kefalas P, Kanellis AK, Roussis V, Makris AM, Kampranis SC. Efficient diterpene production in yeast by engineering Erg20p into a geranylgeranyl diphosphate synthase. Metab Eng. 2015;27:65–75.
30. Tokuhiro K, Muramatsu M, Ohto C, Kawaguchi T, Obata S, Muramoto N, Hirai M, Takahashi H, Kondo A, Sakuradani E, Shimizu S. Overproduction of geranylgeraniol by metabolically engineered *Saccharomyces cerevisiae*. Appl Environ Microbiol. 2009;75:5536–43.
31. Möller S, Croning MDR, Apweiler R. Evaluation of methods for the prediction of membrane spanning regions. Bioinformatics. 2001;17:646–53.
32. Park J, Kang DH, Woo HM. Microbial bioprocess for extracellular squalene production and formulation of nanoemulsions. ACS Sustain Chem Eng. 2021;9:14263–76.
33. Park J, Woo HM. Co-production of l-Lysine and heterologous squalene in CRISPR/dCas9-Assisted *Corynebacterium glutamicum*. J Agric Food Chem. 2022;70:14755–60.
34. Heider SAE, Wolf N, Hofemeier A, Peters-Wendisch P, Wendisch VF. Optimization of the IPP precursor supply for the production of lycopene, Decaprenoxanthin and Astaxanthin by *Corynebacterium glutamicum*. Front Bioeng Biotechnol. 2014;2:28.
35. Lim H, Park J, Woo HM. Overexpression of the key enzymes in the Methylerythritol 4-phosphate pathway in *Corynebacterium glutamicum* for improving Farnesyl Diphosphate-Derived terpene production. J Agric Food Chem. 2020;68:10780–6.
36. Heider SAE, Peters-Wendisch P, Beekwilder J, Wendisch VF. IdsA is the major geranylgeranyl pyrophosphate synthase involved in carotenogenesis in *Corynebacterium glutamicum*. FEBS J. 2014;281:4906–20.
37. Leonard E, Ajikumar PK, Thayer K, Xiao W-H, Mo JD, Tidor B, Stephanopoulos G, Prather KLJ. Combining metabolic and protein engineering of a terpenoid biosynthetic pathway for overproduction and selectivity control. Proc Natl Acad Sci. 2010;107:13654–9.
38. Lim HN, Lee Y, Hussein R. Fundamental relationship between Operon organization and gene expression. Proc Natl Acad Sci. 2011;108:10626–31.
39. Bathe U, Frolov A, Porzel A, Tissier A. CYP76 oxidation network of abietane diterpenes in lamiaceae reconstituted in yeast. J Agric Food Chem. 2019;67:13437–50.
40. Cheng T, Zhao G, Xian M, Xie C. Improved cis-Abienol production through increasing precursor supply in *Escherichia coli*. Sci Rep 2020, 10.
41. Nowrouzi B, Li RA, Walls LE, d'Espaux L, Malcı K, Liang L, Jonguitud-Borrego N, Lerma-Escalera AI, Morones-Ramirez JR, Keasling JD, Rios-Solis L. Enhanced production of taxadiene in *Saccharomyces cerevisiae*. Microb Cell Fact. 2020;19:200.
42. Walter T, Veldmann KH, Götker S, Busche T, Rückert C, Kashkooli AB, Paulus J, Cankar K, Wendisch VF. Physiological response of Corynebacterium glutamicum to Indole. Microorganisms 2020, 8.
43. Du Z, Peng Z, Yang H, Wu H, Sun J, Huang L. Identification and functional characterization of three cytochrome P450 genes for the abietane diterpenoid biosynthesis in Isodon lophanthoides. Planta 2023, 257.
44. Wei S-P, Qian Z-G, Hu C-F, Pan F, Chen M-T, Lee SY, Xia X-X. Formation and functionalization of membraneless compartments in *Escherichia coli*. Nat Chem Biol. 2020;16:1143–8.
45. Wang X, Pereira JH, Tsutakawa S, Fang X, Adams PD, Mukhopadhyay A, Lee TS. Efficient production of oxidized terpenoids via engineering fusion proteins of terpene synthase and cytochrome P450. Metab Eng. 2021;64:41–51.

Publisher's note